# A CFD-DEM-IBM Method for Cartesian Grid Simulation of Gas-Solid Flow in Complex Geometries

**Peng Zhao, Ji Xu, Wei Ge and Junwu Wang**

**State Key Laboratory of Multiphase Complex Systems, Institute of Process Engineering, Chinese Academy of Sciences**

# Content

- Background
- CFD-DEM-IBM Method
- Simulation Result
- Conclusion

# Fluidized bed in industrial applications

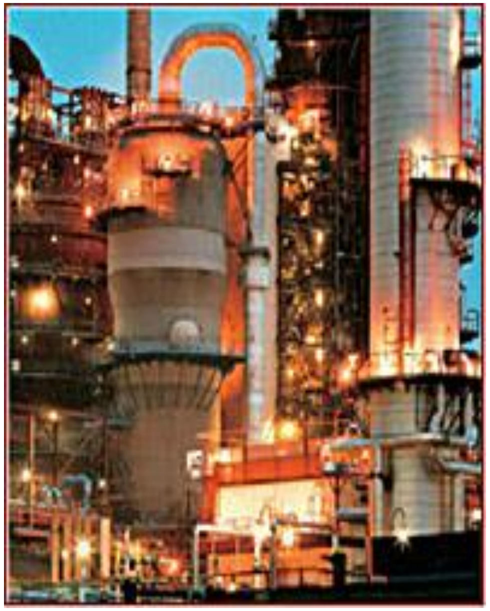

Petroleum catalytic cracking

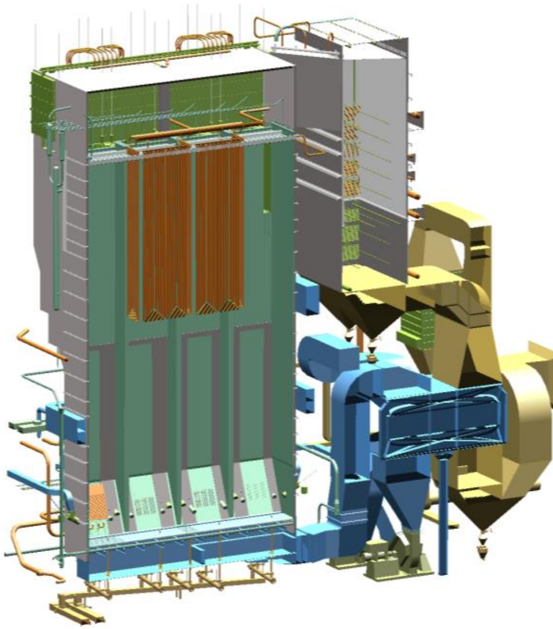

Coal fired boiler

Ore Roasting

**Fluidized beds with complex geometries are ubiquitous in industrial applications**

# Multiscale Simulation of Fluidization

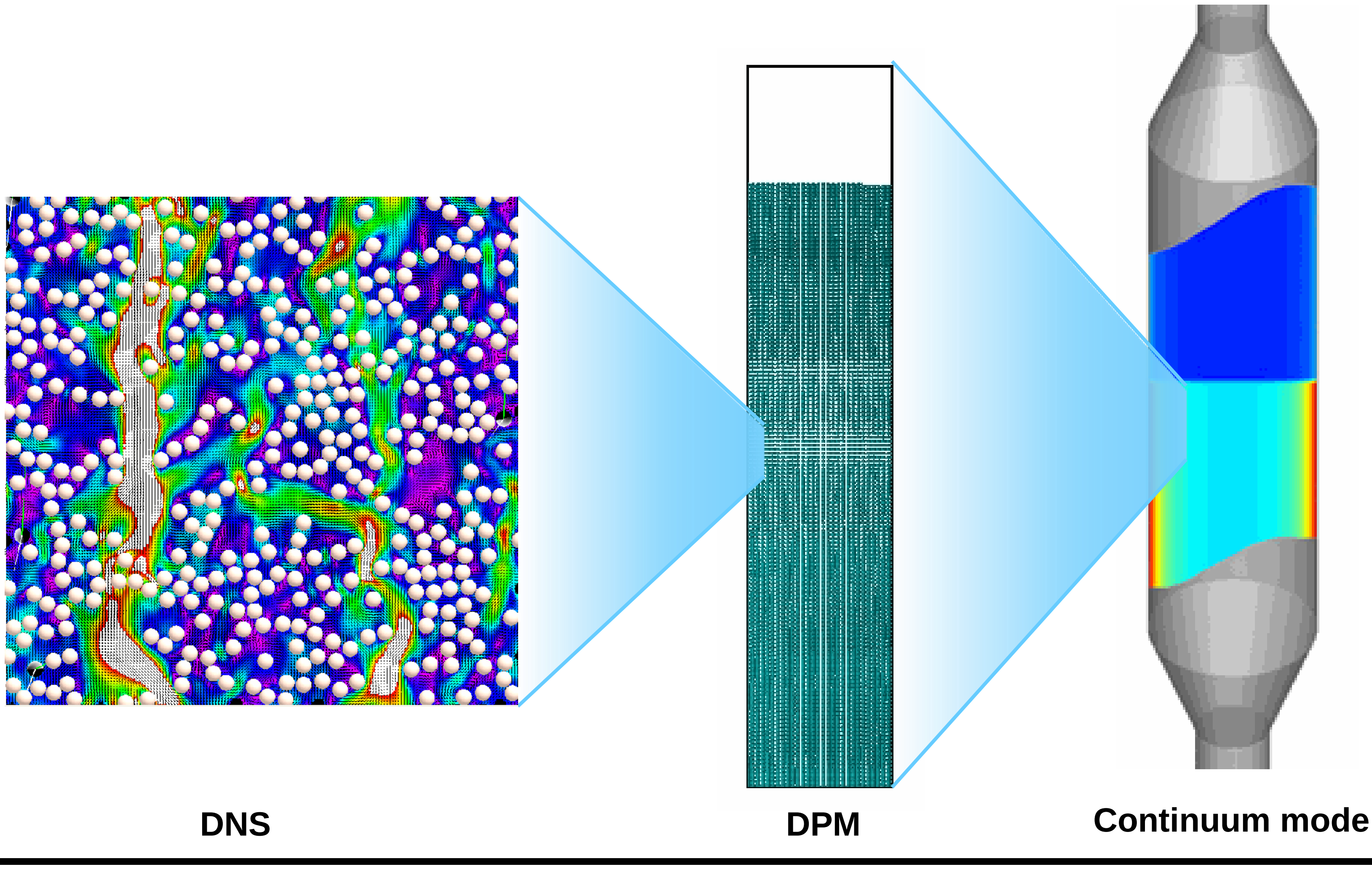


**Larger scale, less details and computational cost**

van der Hoef et al., *Advances in Chemical Engineering*. 2006, 31: 65-149

# Unstructured VS. Cartesian grids

| | | Grid generation | Grid quality | mapping the information between two phases |
|---|---|---|---|---|
| **Unstructured** |  | Complicated, time-consuming | Low | Difficult |
| **Cartesian** |  | Simple | High | Exact and analytical |

**Cartesian-grid-based (coarse-grained) CFD-DEM-IBM method for modeling gas-solid flows in complex geometries**

Mittal, R., Iaccarino, G., 2005. Annual Review of Fluid Mechanics 37, 239-261.
Kuang, S., Yu, A., Zou, Z., 2008. International Journal of Multiphase Flow34 (11), 1023–1030.

# CFD-DEM-IBM method

**CFD-DEM-IBM method**

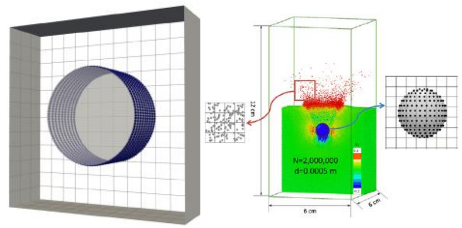

De Jong et al., Chemical Engineering Science 2012, 84, 814–821
De Jong et al., Chemical Engineering Science 2012, 84, 822–833
Xu et al., Chemical Engineering Science 2013, 104, 201–207

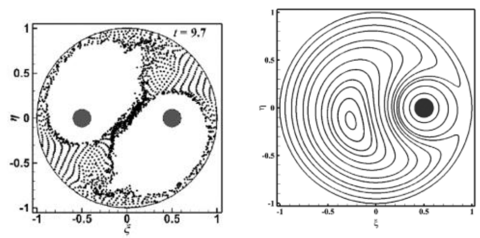


Ku et al., International Journal of Multiphase Flow 2016, 87, 80–89
Ku et al., International Journal of Multiphase Flow 2018, 103, 124-140
Ku et al., International Journal of Multiphase Flow 2019, 113, 71 – 88

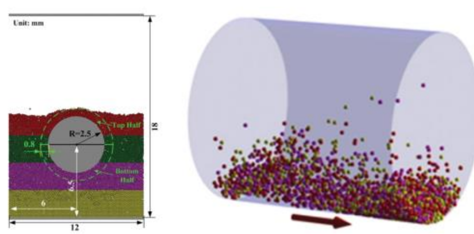


Guo et al., AIChE Journal 2013, 59, 1075–1087

**Can not maintain the sharpness of boundaries due to the use of discrete delta function**

# Content

- Background
- CFD-DEM-IBM Method
- Simulation Result
- Conclusion

# CFD-DEM Method

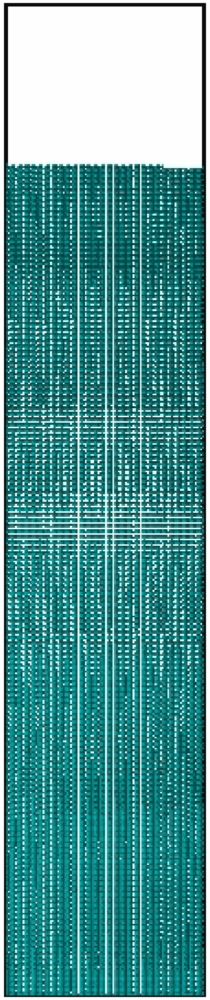

**Volume-averaged Navier-Stokes equations for gas phase:**

$$\frac{\partial}{\partial t}(\varepsilon_g \rho_g) + \nabla \cdot (\varepsilon_g \rho_g \mathbf{V}_g) = 0$$

$$\frac{\partial}{\partial t}(\varepsilon_g \rho_g \mathbf{V}_g) + \nabla \cdot (\varepsilon_g \rho_g \mathbf{V}_g \mathbf{V}_g) = -\varepsilon_g \nabla p + \nabla \cdot \boldsymbol{\tau}_g + \varepsilon_g \rho_g \mathbf{g} - \mathbf{F}_{drag}$$

**Particle dynamics:**

$$\frac{d}{dt}(I_p \overline{\omega}_p) = \overline{T}$$

$$m_a \frac{d\,\mathrm{v}_a}{dt} = -V_a \nabla p + F_{drag,a} + m_a \mathrm{g} + \mathrm{F}_{c,a}$$ ← Linear DEM

**Interphase drag force:**

$$\mathbf{F}_{drag} = \frac{1}{V_{cell}} \sum_{\forall a \in cell} \frac{\beta V_a}{1-\varepsilon_g} (\mathbf{V}_g - \mathbf{V}_a) \delta(r - r_a)$$

Deen et al., Chem. Eng. Sci. 2007, 62, 28-44. van der Hoef et al., Adv. Chem. Eng. 2006, 31, 65-149.

# Immersed boundary method

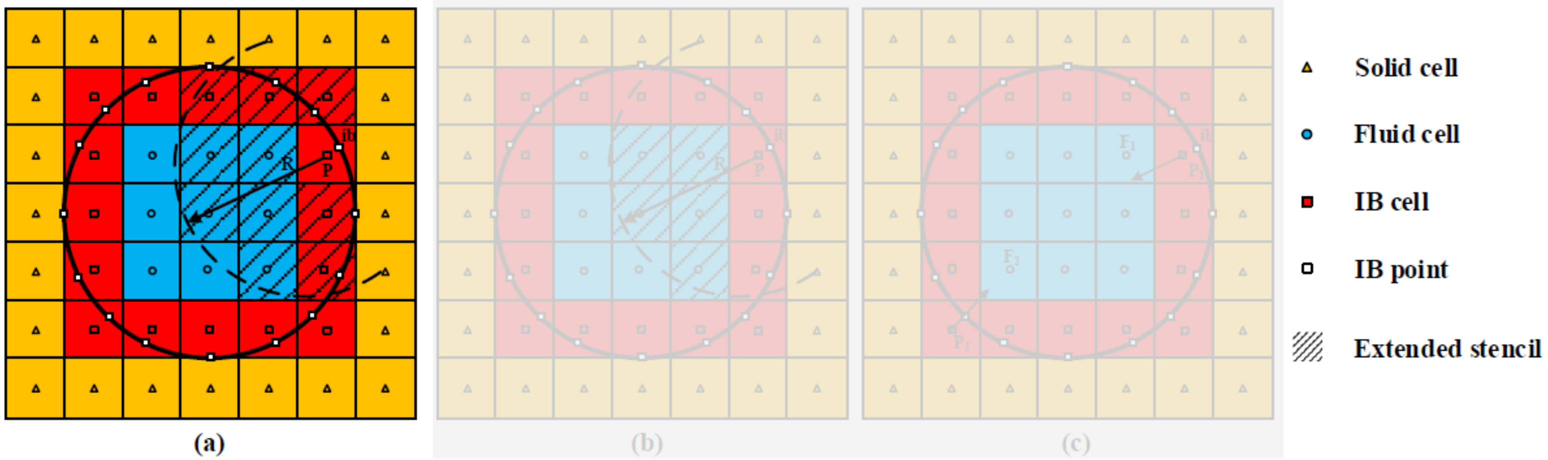


**Figure 1**:The local reconstruction scheme: (a) the second-order polynomial in OpenFOAM, (b) the second-order polynomial in present study, (c) the zero-gradient Neumann BC in present study

- **Second-order interpolated reconstructed method in OpenFOAM**

As shown in sub-figure (a), a second-order interpolated polynomial of $\Phi$ is used to approximate a generic variable $\varphi$ in the vicinity of IB points $(x_{ib}, y_{ib}, z_{ib})$:

$$\varphi(x,y,z) \approx \Phi(x,y,z) = \sum_{i=0}^{N}\sum_{j=0}^{N}\sum_{k=0}^{N} c_{ijk}\left(x-x_{ib}\right)^{i}\left(y-y_{ib}\right)^{j}\left(z-z_{ib}\right)^{k} \quad i+j+k \le 2$$

The unknown coefficients $c_{ijk}$ are determined using the weighted least square method on extended stencil, and substituted into equation at IB cells, the values of $\varphi$ IB cells can then be obtained.

**Drawback: other IB cells are included in extended stencil, thus iterations are needed**

Tukovic, Z., Jasak, H., 2012. Immersed boundary method in OpenFOAM, 7th OpenFOAMr Workshop, pp. 25–28.
Mittal, R., Dong, H., Bozkurttas, M., Najjar, F.M., Vargas, A., von Loebbecke, A., 2008. Journal of Computational Physics 227, 4825-4852.
Seo, J.H., Mittal, R., 2011. Journal of Computational Physics 230, 1000-1019.

# Immersed boundary method

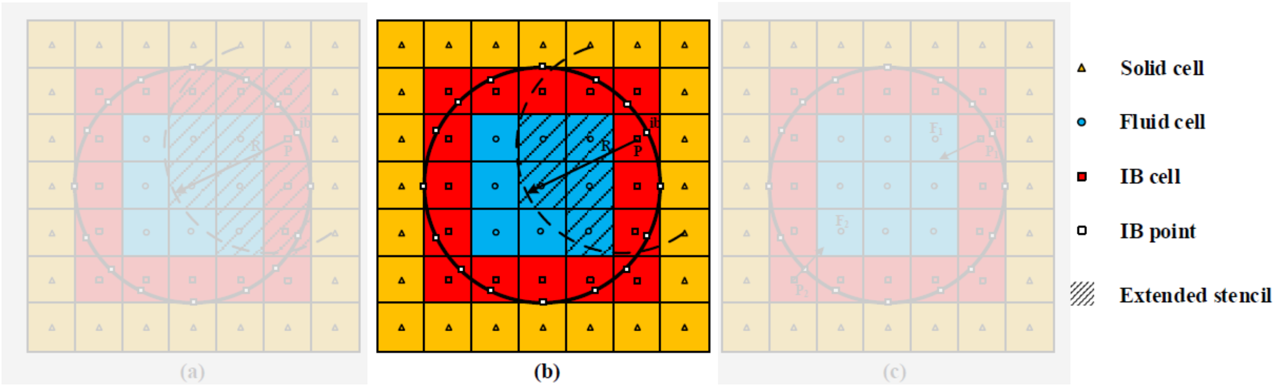


- **Second-order interpolated reconstructed method in present study**
  The neighboring IB cells were not included in the interpolated extended stencil, therefore, iterations are not needed during imposing BCs.

Tseng, Y.-H., Ferziger, J.H., 2003.Journal of Computational Physics 192, 593-623.
Seo, J.H., Mittal, R., 2011. Journal of Computational Physics 230, 1000-1019.

# Immersed boundary method

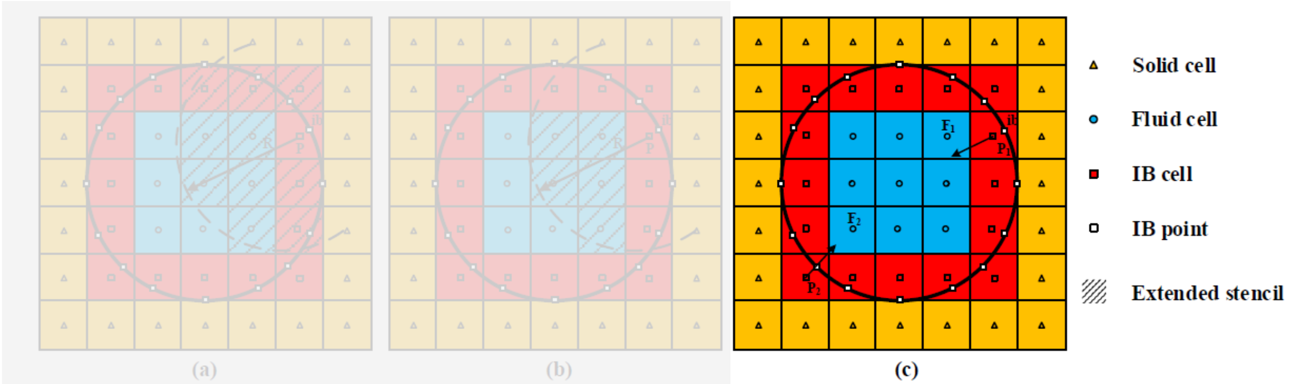


- **Second-order interpolated reconstructed method in present study**

  The neighboring IB cells were not included in the interpolated extended stencil, therefore, iterations were not needed during imposing BCs.

- **First-order zero-gradient method**

  Setting the value of flow variables($\varphi$) in IB cell equals to the closet fluid cell in the normal direction: $\varphi_{P1(2)} = \varphi_{F1(2)}$ , the normal gradient in IB point was approximately supposed to be zero.

  **Drawback: only applicable to small gradients**

**Table 1:** Four different BC imposition methods on immersed interfaces

| Case | 1 | 2 | 3 | 4 |
|---|---|---|---|---|
| U | a | a | b | b |
| p | a | c | b | c |

Tseng, Y.-H., Ferziger, J.H., 2003.Journal of Computational Physics 192, 593-623.
Seo, J.H., Mittal, R., 2011. Journal of Computational Physics 230, 1000-1019.

# Content

- Background
- CFD-DEM-IBM Method
- Simulation Result
- Conclusion

# Bubbling fluidized bed

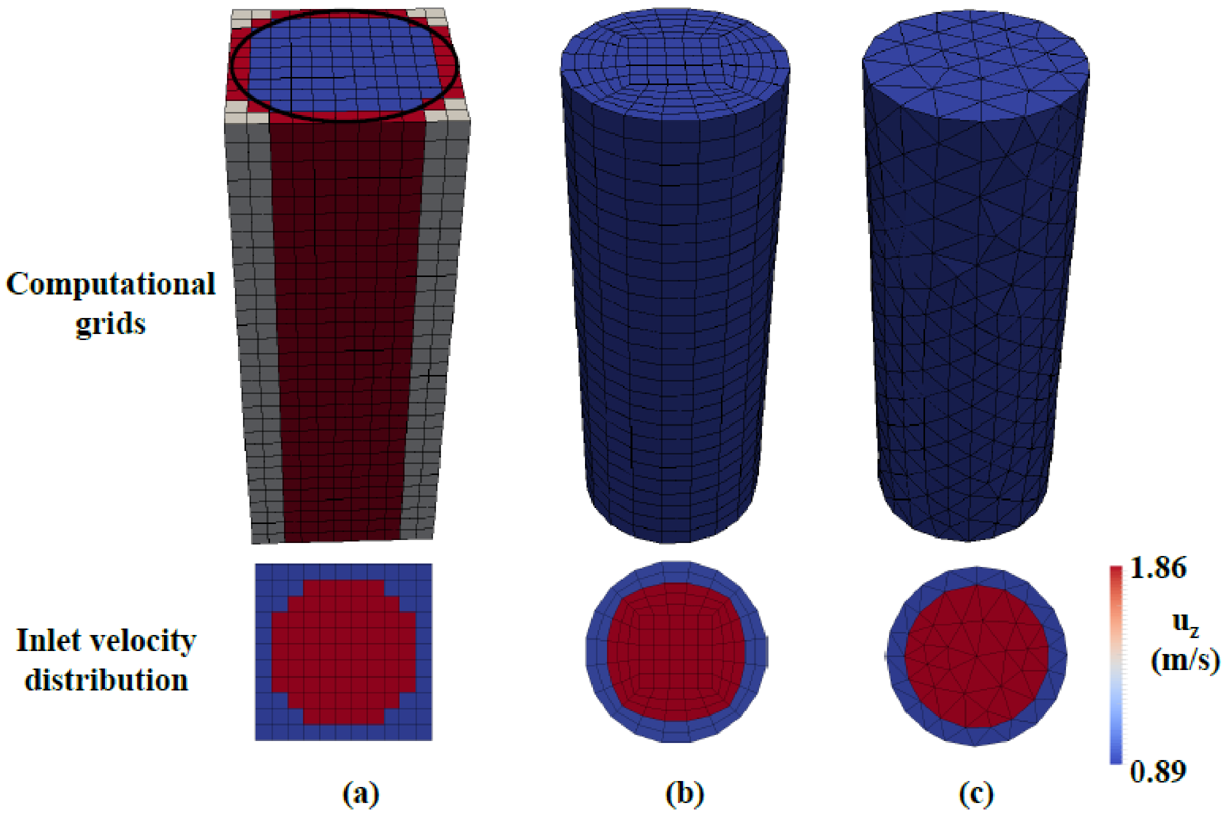


**Figure 2**: The Cartesian (cube) (a), structured (hexahedron) (b) and unstructured (tetrahedron) (c) fluid grids and the corresponding distribution of inlet velocity of fluidized bed

Holland, D.J., Müller, C.R., Dennis, J.S., Gladden, L.F., Sederman, A.J., 2008. Powder Technology 182, 171-181.

# Bubbling fluidized bed

**Table 2**: Physical and numerical parameters in cylindrical bubbling fluidized bed

| Parameter | Value |
|---|---|
| Gas phase | |
| Initial pressure, p (Pa) | $10^5$ |
| Temperature, T (K) | 298.15 |
| Inlet superficial velocity, u (m/s) | 0.6 |
| Inlet voidage, $\varepsilon$ | 0.4 |
| CFD time step, dt (s) | $1.25 \times 10^{-4}$ |
| Particles | |
| Particle dynamics time step (s) | $1.25 \times 10^{-5}$ |
| Diameter of particles, $d_p$ (mm) | 1.2 |
| Density of particles, $\rho_p$ (kg/$m^3$) | 900 |
| Number of particle, $N_{part}$ | 30325 |
| Normal spring stiffness, $k_n$ (N/m) | 3000 |
| Tangential spring stiffness, $k_t$ (N/m) | 428 |
| Friction coefficient, $\mu_f$ | 0.1 |
| Restitution coefficient, $e_n$,$e_t$ | 0.95 |
| Geometry | |
| High of bed, $H_{bed}$ (mm) | 120 |
| Diameter of bed, $d_{bed}$ (mm) | 44 |
| Cartesian grid length (m) | 0.004 |

# Bubbling fluidized bed

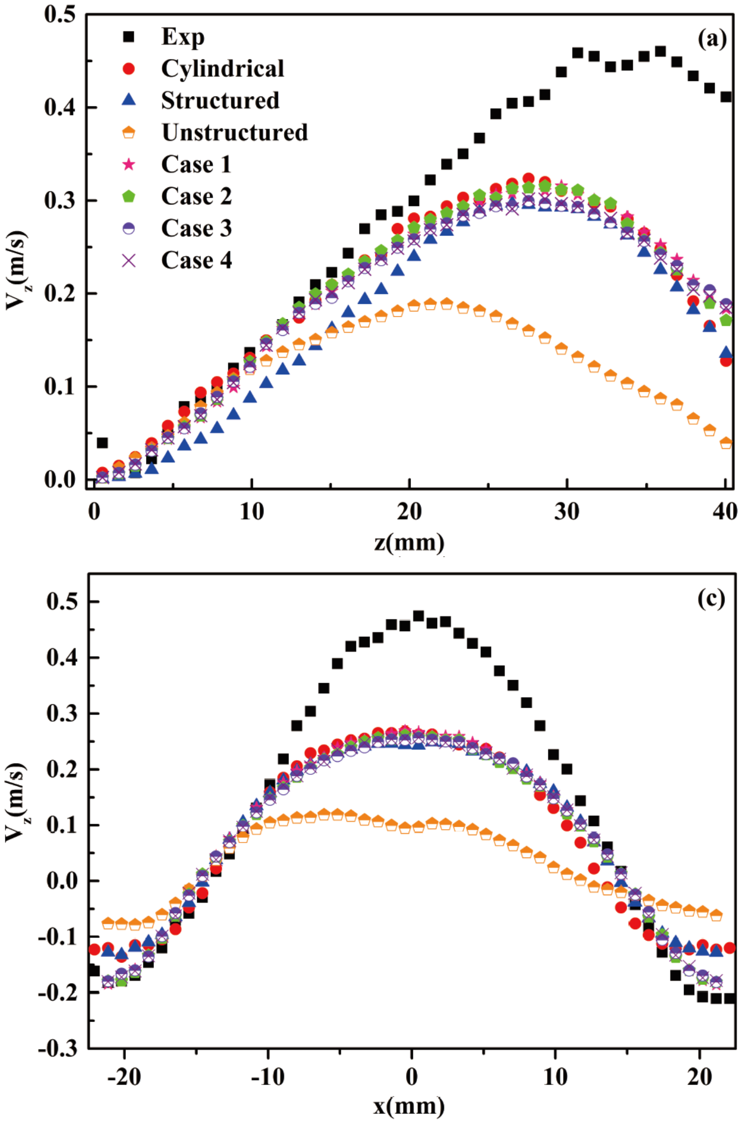


**Figure 3**: The time-averaged axial particle velocity (m/s) with experiment and simulation under different grid types along (a) a vertical slice at the x-direction centerline, (b) a horizontal slice 20mm above the distributor and (c) a horizontal slice 35mm above the distributor. The grid types including: cylindrical (Boyce et al., 2013), structured, unstructured and Cartesian grid (cases 1-4).


Holland, D.J., Müller, C.R., Dennis, J.S., Gladden, L.F., Sederman, A.J., 2008. Powder Technology 182, 171-181.
Boyce, C.M., Holland, D.J., Scott, S.A., Dennis, J.S., 2013. Industrial & Engineering Chemistry Research 52, 18085-18094.

# Bubbling fluidized bed

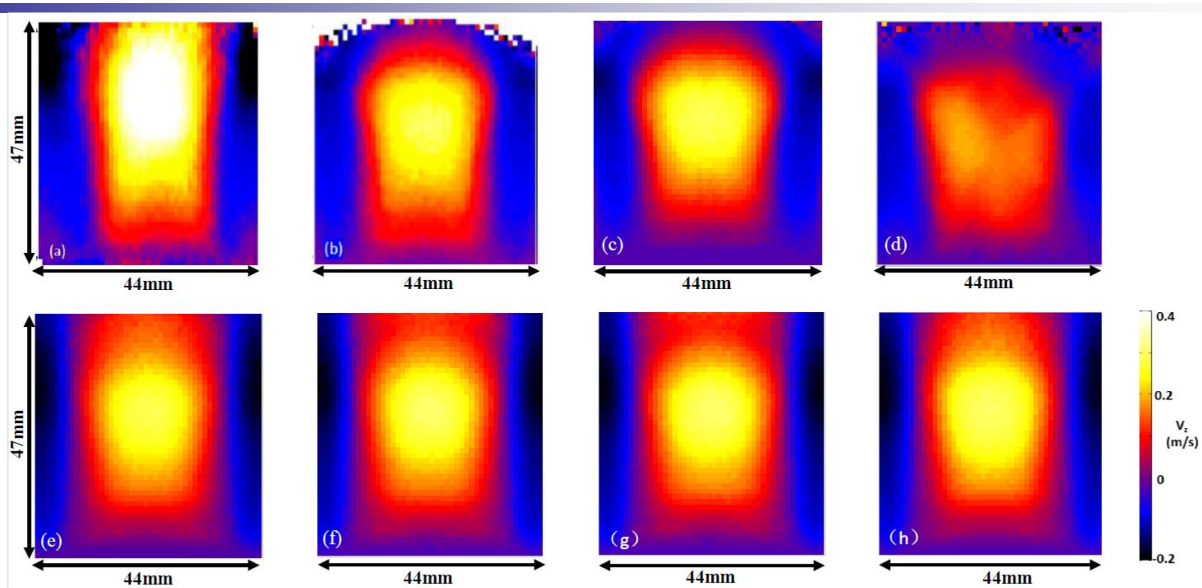


**Figure 4**: The time-averaged axial particle velocity image from (a) experimental MR imaging (Holland et al., 2008), (b) cylindrical grid CFD-DEM simulation (Boyce et al., 2013), (c) structured grid CFD-DEM simulation, (d) unstructured grid CFD-DEM simulation, (e-h) Cartesian grid CFD-DEM simulation and the interactions of fluid and cylindrical wall were described by cases 1-4, respectively.

**Table 3:** The number of computational grids and the elapsed CPU time for 20 s real time under different grid types and BC imposition methods on immersed interfaces

| | **Case 1** | **Case 2** | **Case 3** | **Case 4** | **Structured** | **Unstructured** |
|---|---|---|---|---|---|---|
| Number of grids | 3270 | 3270 | 3270 | 3270 | 3250 | 3264 |
| CPU time(s) | 391856 | 10907 | 11136 | 6255 | 6155 | 16437 |

Holland, D.J., Müller, C.R., Dennis, J.S., Gladden, L.F., Sederman, A.J., 2008. Powder Technology 182, 171-181.
Boyce, C.M., Holland, D.J., Scott, S.A., Dennis, J.S., 2013. Industrial & Engineering Chemistry Research 52, 18085-18094.

# Bubbling fluidized bed with tubes

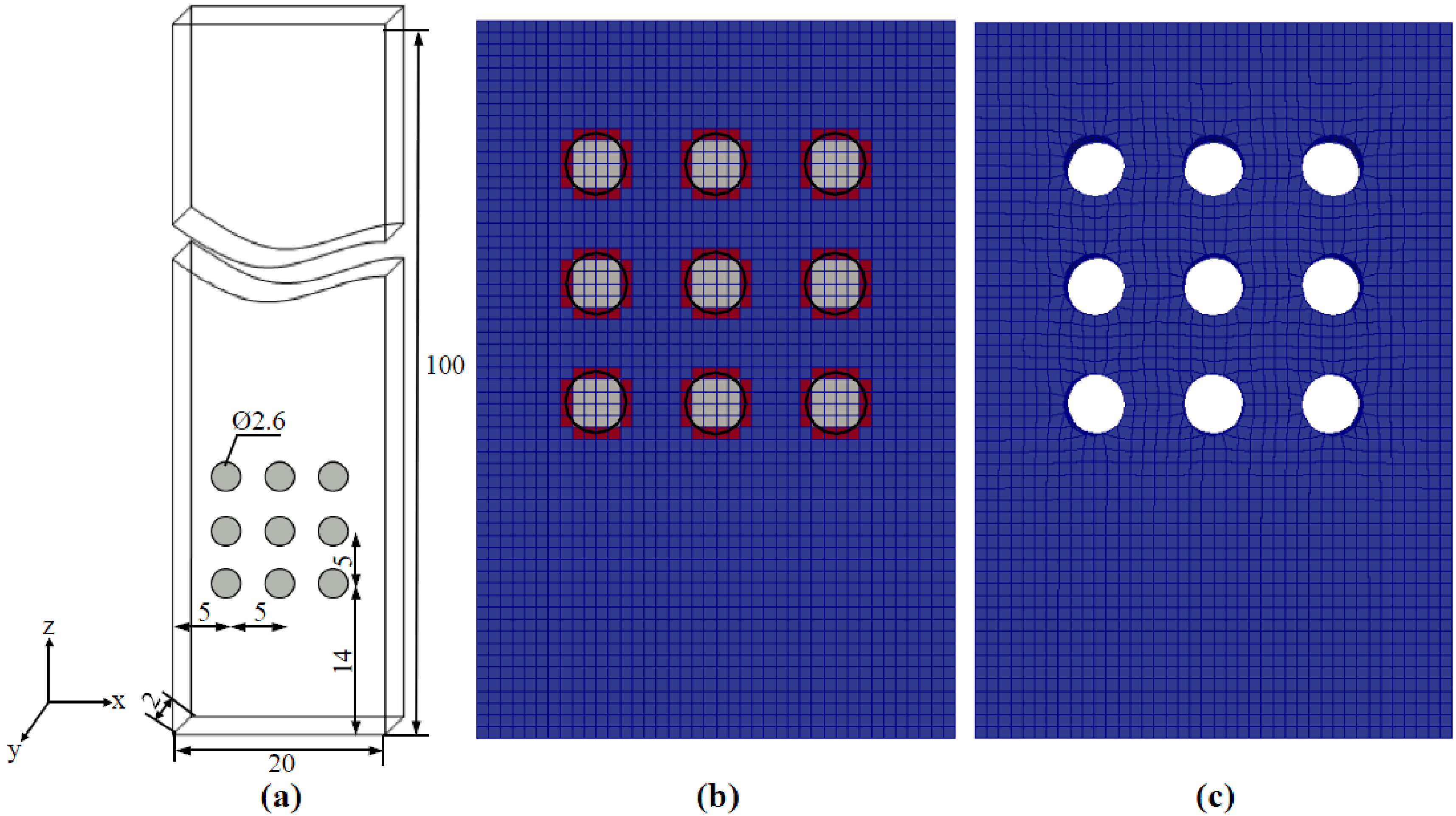


**Figure 5:** Geometrical description and local grids around immersed tube bundle: (a) sketch of the bed, (b) Cartesian grids and (c) unstructured grids.

Yang, S., Luo, K., Fan, J., Cen, K., 2014. Industrial & Engineering Chemistry Research 53, 6896-6912.

# Bubbling fluidized bed with tubes

**Table 4:** Physical and numerical parameters for simulating the bubbling fluidized bed with immersed tubes

| Parameter | Value |
|---|---|
| Gas phase | |
| Temperature, T (K) | 298 |
| Viscosity, $\mu$ (Pa s) | $1.85\times10^{-5}$ |
| Inlet superficial gas velocity, u (m/s) | 0.15 |
| Molecular weight, M (g/mol) | 28.8 |
| Pressure, p (atm) | 1.0 |
| Density, $\rho_g$ (kg/$m^3$) | 1.205 |
| CFD time step, dt (s) | $1.0\times10^{-5}$ |
| Particles | |
| Number of particle | 99560 |
| Diameter, $d_p$ (mm) | 0.23 |
| Density, $\rho_p$ (kg/$m^3$) | 2700 |
| Normal spring stiffness, $k_n$ (N/m) | 5000 |
| Tangential spring stiffness, $k_t$ (N/m) | 714.3 |
| Friction coefficient | 0.3 |
| Restitution coefficient, $e_n, e_t$ | 0.97 |
| Rolling friction coefficient | 0.01 |
| Particle dynamics time step (s) | $5.0\times10^{-7}$ |
| Geometry | |
| Width, $x$ (mm) | 20 |
| Thickness, $y$ (mm) | 2 |
| Height, $z$ (mm) | 100 |
| Cartesian grid length (mm) | 0.5 |
| Tube diameter (mm) | 2.6 |

# Bubbling fluidized bed with tubes

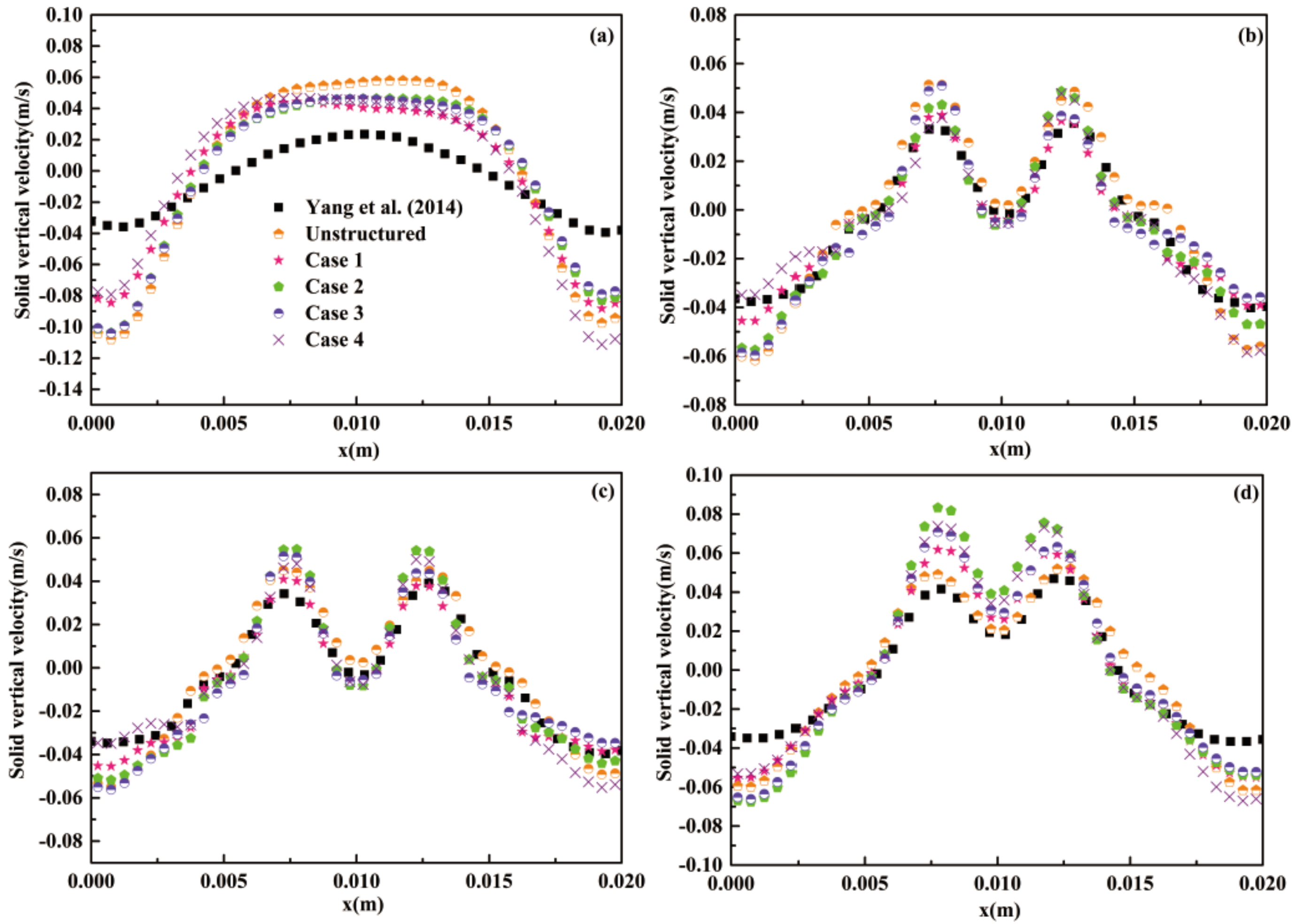


**Figure 6**: Comparison of the time-averaged axial particle velocity (m/s) using unstructured and Cartesian grids (cases 1-4) with the simulation results of Yang et al. (2014): (a) z = 0.007 m; (b) z = 0.017 m; (c) z = 0.022 m; (d) z = 0.027 m.



Yang, S., Luo, K., Fan, J., Cen, K., 2014. Industrial & Engineering Chemistry Research 53, 6896-6912.

# Bubbling fluidized bed with tubes

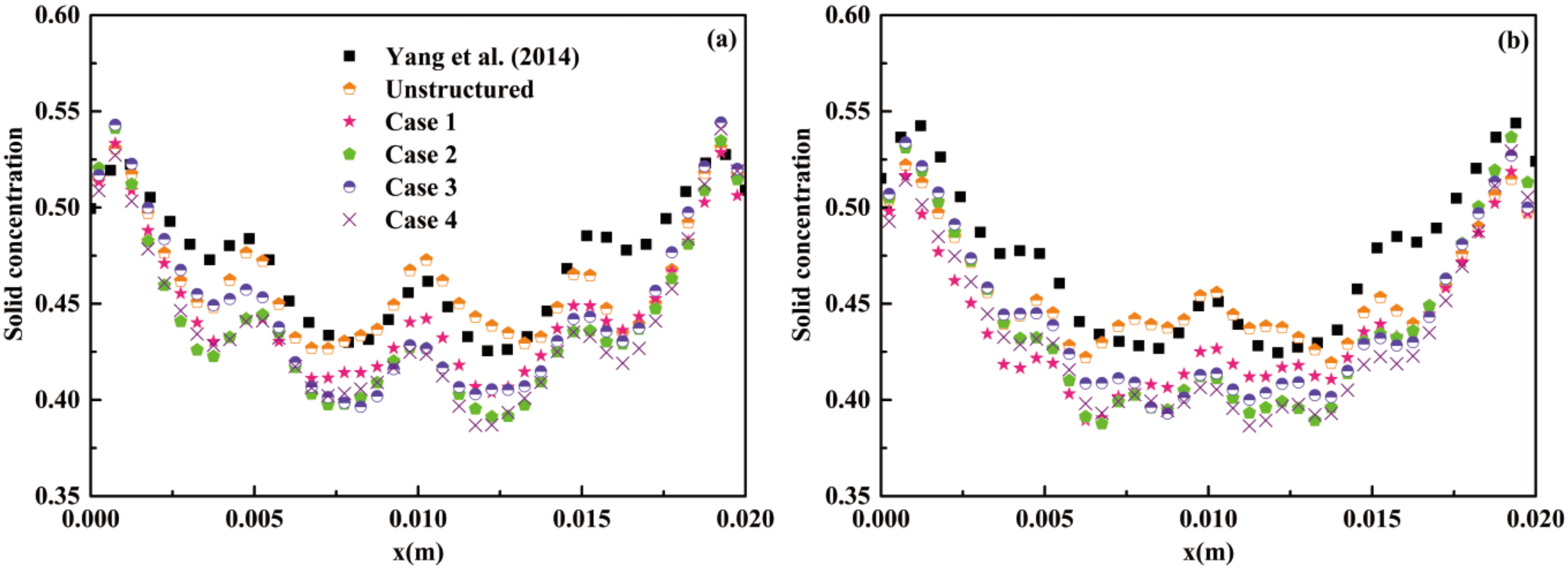


**Figure 9**: Comparison of the time-averaged particle concentration using unstructured and Cartesian (cases 1-4) grids: (a) Cartesian grids: z = 0.0165 m, unstructured grids: z = 0.017 m; (b) Cartesian grids: z = 0.0215 m, unstructured grids: z = 0.022 m.

**Table 5:** The number of computational grids and elapsed CPU time for 20 s real time under different grid types and BC imposition methods on immersed interfaces

| | Case 1 | Case 2 | Case 3 | Case 4 | Unstructured |
|---|---|---|---|---|---|
| Number of grids | 31856 | 31856 | 31856 | 31856 | 31232 |
| CPU time(s) | 1635620 | 361885 | 357548 | 341537 | 523712 |

# Content

- Background
- CFD-DEM-IBM Method
- Simulation Result
- Conclusion

# Conclusion

- A CFD-DEM-IBM method was proposed for modeling gas-solid flow in complex geometries

- The simulation results agree well with the reported experimental and numerical data available in literature

- The proposed CFD-DEM-IBM method is one or two orders of magnitude faster than that of the original IBM of Tukovic and Jasak (2012) in OpenFOAM

# Acknowledgement

- National Natural Science Foundation of China (91834303)

- Key Research Program of Frontier Science, Chinese Academy of Sciences (QYZDJ-SSW-JSC029)

- Transformational Technologies for Clean Energy and Demonstration, Strategic Priority Research Program of the Chinese Academy of Sciences (XDA21030700)